Synthesis of 2,4-Diamino-6-[2′-*O*-(ω-carboxyalkyl)oxydibenz[*b*,*f*]azepin-5-yl]-methylpteridines as Potent and Selective Inhibitors of *Pneumocystis carinii*, *Toxoplasma gondii*, and *Mycobacterium avium* Dihydrofolate Reductase

Andre Rosowsky,*[,†] Hongning Fu,[†] David C. M. Chan,[†] and Sherry F. Queener[‡]

Dana-Farber Cancer Institute and Department of Biological Chemistry and Molecular Pharmacology, Harvard Medical School, Boston, Massachusetts 02115, and Department of Pharmacology and Toxicology, Indiana University School of Medicine, Indianapolis, Indiana 46202

Received November 26, 2003

Six previously undescribed *N*-(2,4-diaminopteridin-6-yl)methyldibenz[*b*,*f*]azepines with water-solubilizing *O*-carboxyalkyloxy or *O*-carboxybenzyloxy side chains at the 2′-position were synthesized and compared with trimethoprim (TMP) and piritrexim (PTX) as inhibitors of dihydrofolate reductase (DHFR) from *Pneumocystis carinii* (Pc), *Toxoplasma gondii* (Tg), and *Mycobacterium avium* (Ma), three of the opportunistic organisms known to cause significant morbidity and mortality in patients with AIDS and other disorders of the immune system. The ability of the new analogues to inhibit reduction of dihydrofolate to tetrahydrofolate by Pc, Tg, Ma, and rat DHFR was determined, and the selectivity index (SI) was calculated from the ratio IC_{50}(rat DHFR)/IC_{50}(Pc, Tg, or Ma DHFR). The IC_{50} values of the 2′-*O*-carboxypropyl analogue (**10**), with SI values in parentheses, were 1.1 nM (1300) against Pc DHFR, 9.9 nM (120) against Tg DHFR, and 2.0 nM (600) against Ma DHFR. The corresponding values for the 2′-*O*-(4-carboxybenzyloxy) analogue (**12**) were 1.0 nM (560), 22 nM (21), and 0.75 nM (630). By comparison, the IC_{50} and SI values for TMP were Pc, 13 000 nM (14); Tg, 2800 nM (65); and Ma, 300 nM (610). For the prototypical potent but nonselective inhibitors PTX and TMX, respectively, these values were Pc, 13 nM (0.26) and 47 nM (0.17); Tg, 4.3 nM (0.76) and 16 nM (0.50); Ma, 0.61 nM (5.4) and 1.5 nM (5.3). Thus **10** and **12** met the criterion for DHFR inhibitors that combine the high selectivity of TMP with the high potency of PTX and TMX.

Introduction

Despite the considerable number of active new antiretroviral agents and a growing understanding of the origin and potential means of circumvention of drug resistance to these agents, typically through the use of multidrug cocktails,[1,2] major progress in the treatment of AIDS has thus far been confined to the economically most affluent countries of the world. As a result of limited access to these often very costly antiviral medications in underdeveloped nations,[3] disabling and often life-threatening opportunistic infections by various parasites to which AIDS patients are especially vulnerable[4] are a global public health concern with major social and political implications.[5] Among the more prevalent of these infections, and indeed in some cases the earliest event signaling T-cell destruction by the HIV-1 or HIV-2 virus, are those caused by the opportunistic organisms *Pneumocystis carinii* (Pc),[6] *Toxoplasma gondii* (Tg),[7,8] *Mycobacterium avium* (Ma),[9] and *Cryptosporidium parvum* (Cp),[10] to name just four. Because of the severe impact that infections by these often coexisting parasites can have on the duration and quality of life of AIDS patients, and because a general concensus is lacking as to the proper length of treatment with antiparasitic drugs once intensive multidrug anti-HIV therapy has brought down the number of virus particles in the blood to very low levels, efforts are continuing to find newer agents that can complement the currently available drugs for treatment and/or prophylaxis of HIV-associated opportunistic infections.

Our laboratory[11] and others[12−15] have been engaged since the early 1990s in the design and synthesis of small-molecule inhibitors of dihydrofolate reductase (DHFR), in the hope of finding agents that would be superior to two-drug antifolate regimens combining, for example, an inhibitor of dihydropteroate synthetase (e.g., sulfamethoxazole or dapsone) with a DHFR inhibitor such as trimethoprim (**1**) or pyrimethamine (**2**).[16] Coadministration of the sulfa drug is typically required in the case of trimethoprim because the latter, when given alone, is not potent enough to completely eradicate the infection. However many patients develop severe allergic skin reactions to sulfa drugs[17] and therefore have to discontinue treatment before a complete cure is achieved. Furthermore, given the fact that only mutations in dihydropteroate synthetase, and not DHFR, have been observed in resistant Pc strains, investigators are beginning to question the role of trimethoprim in co-trimoxazole (trimethoprim + sulfamethoxazole), the two-drug combination almost universally prescribed for Pc prophylaxis.[18] A much more potent DHFR inhibitor than trimethoprim, approved a few years ago for use in AIDS patients suffering from *Pneumocystis carinii* pneumonia, is trimetrexate (**3**).[19] Unlike trimethoprim, which is much more selective in its ability to bind selectively to Pc DHFR and other opportunistic para-

* To whom correspondence should be addressed. Phone: 617-632-3117. Fax: 617-632-2410. E-mail: andre_rososwky@dfci.harvard.edu.
† Dana-Farber Cancer Institute.
‡ Indiana University.

10.1021/jm030599o CCC: $27.50
Published on Web 04/10/2004

sites as compared with human DHFR, trimetrexate lacks this selectivity and therefore requires coadministration of leucovorin (5-formyltetrahydrofolic acid) to *selectively protect the patient* from severe hematologic side effects that would otherwise occur. Piritrexim (**4**)

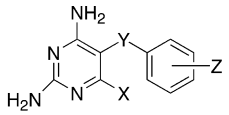

1 : X = H, Y = CH_2, Z = 3,4,5-$(OMe)_3$
2 ; X = Et, Y = none, Z = 4-Cl

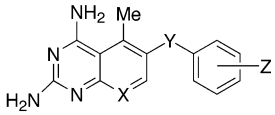

3 : X = CH, Y = CH_2NH, Z = 3,4,5-$(OMe)_3$
4 : X = N, Y = CH_2, Z = 2,5-$(OMe)_2$

closely resembles trimetrexate in that it has very high affinity for DHFR, but lacks selectivity and thus requires leucovorin coadministration.[20] The explanation generally given for this selectivity of protection is that the parasites synthesize their own reduced folate cofactors de novo and therefore, in contrast to mammalian cells, have no need for folate transporter proteins in their cell membrane.[21] Given the limitations of both the trimethoprim/sulfa and trimetrexate/leucovorin regimens mentioned above, a single DHFR inhibitor combining the potency of trimetrexate (or piritrexim) with the species selectivity of trimethoprim would be desirable, in that it would eliminate the need to coadminister either a sulfa drug or leucovorin.

In 1999 we reported the synthesis of a novel group of 2,4-diaminopteridine DHFR inhibitors containing a lipophilic tricyclic group at the 6-position, as exemplified by general structure **5**.[22] The most interesting member of the series was the dibenz[*b*,*f*]azepine **6**, whose potency

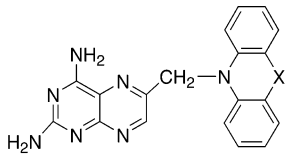

5 : X = 0-2 atoms
6 : X = -CH=CH

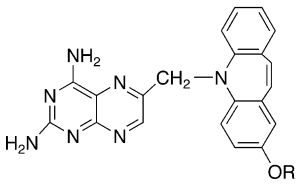

7 : R = H
8 : R = CH_2COOH
9 : R = $(CH_2)_2COOH$
10 : R = $(CH_2)_3COOH$
11 : R = $(CH_2)_4COOH$
12 : R = $CH_2C_6H_4$(4-COOH)

and selectivity against Pc DHFR were only moderate, but whose potency against Tg DHFR approached that of trimetrexate. Moreover, while trimetrexate was a better inhibitor of the mammalian DHFR (in this case the rat enzyme) and thus was completely devoid of selectivity, **6** showed a 100-fold binding preference for Tg DHFR. Compound **6** was also several times more potent and selective against Ma DHFR than rat DHFR and was a much better inhibitor of both Tg and Ma DHFR than trimethoprim. In a subsequent study, the 3D structure of the ternary complex of **6** and NADPH with Pc DHFR was analyzed by crystallography, and an unusual role was uncovered for the dibenz[*b*,*f*]-azepine moiety in positioning the diaminopteridine within the active site.[23]

In an assay based on measurement of [^{3}H]uracil incorporation into the DNA of Tg tachyzoites in culture, **6** had an IC_{50} of 0.077 μM[22] and thus was roughly 100 times more potent than pyrimethamine. Reasonable growth inhibition was also observed against intact *P. carinii* organisms grown on monolayers of human embryonic lung fibroblasts (with folic acid present in the medium in order to protect the feeder cells). The IC_{50} of **6** in this assay was estimated to be ca. 2 μM, whereas trimethoprim had essentially no effect.[22] Although the methods used to compare activity against intact Pc and Tg organisms were different, there was reasonable consistency between the DHFR inhibition data on one hand and the growth inhibition data on the other. In sum, **6** appeared to be a promising starting point from which to launch structure−activity optimization with both species, as well as Ma, as targets.

The results with other compounds in our original study[22] suggested that the dibenz[*b*,*f*]moiety might be contributing in a major way to the structure−activity and structure−selectivity profile. An attempt to enhance the potency of **6** by replacing the pteridine ring with a pyrido[2,3-*d*]pyrimidine or quinazoline, or by interchanging the azepine ring nitrogen and CH_2 bridge, did not yield encouraging results.[24] However, we now report that a substantial improvement in potency and selectivity against not only Tg DHFR but also Pc and Ma DHFR can be realized by modifying the 2′-position of the dibenz[*b*,*f*]azepine ring as in structures **7**−**12**. The carboxylic acid side chain in these compounds is also present as a key structural motif in several recently studied 2,4-diamino-5-(2′,5′-disubstituted benzyl)]pyrimidines from this laboratory.[11a,b] The best of the new analogues reported here is 2,4-diamino-6-[2′-*O*-(3-carboxypropyl)oxydibenz-[*b*,*f*]azepin-5-yl]methylpteridine (**10**), which has an IC_{50} of 1.1 nM against Pc DHFR and a remarkable selectivity index of 1300 (95% confidence interval = 850−2000) for Pc versus rat DHFR. Compound **10** is also very potent and selective against Ma DHFR, but is less selective against the Tg enzyme than against the Pc or Ma enzyme. To our knowledge, it is among the most potent and selective inhibitors of Pc DHFR reported to date.

Chemistry

The synthesis of compounds **7**−**12** from dibenz[*b*,*f*]-azepine (iminostilbene, **13**) is depicted in Scheme 1 and required us to prepare the key intermediate 5*H*-dibenz-[*b*,*f*]azepin-2-ol (**15**) which was obtained essentially as described in the literature.[25,26] Oxidation of **13** with potassium nitrosodisulfonate (Fremy's salt) at 5 °C overnight in a mixture of acetone and potassium phosphate buffer adjusted to precisely pH 7.22 afforded the deep-red iminoquinone **14** in 77% yield. Also formed, and easily separated by silica gel chromatography, was a small amount (ca. 10%) of acridine-9-carboxaldehyde, readily identified by the presence in its ^{1}H NMR spectrum of a singlet at δ 11.5 for the aldehyde proton.

Scheme 1[a]

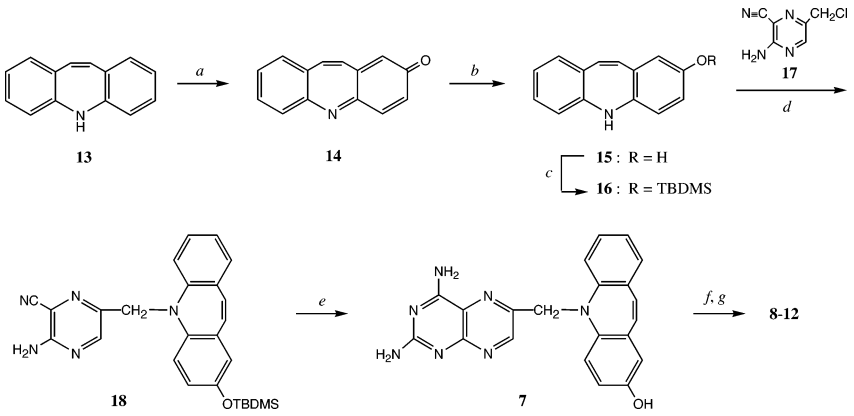

[a] Reagents: (a) Fremy's salt, Na_2HPO_4, aq Me_2CO; (b) $Na_2S_2O_4$, $CHCl_3$; (c) TBDMSCl, Et_3N, $CHCl_3$; (d) **16**, Na_2CO_3, MeCN; (e) $H_2NC(=NH)NH_2$, NaOEt, EtOH; (f) $BrCH_2(X)CO_2Et$, NaOEt, DMSO, or $BrCH_2CO_2H$, DMSO; (g) NaOH.

Some unchanged **13** (ca. 10%) was also recovered and could be recycled. The ^{1}H NMR spectrum of purified **14** featured a well-defined pair of doublets at δ 7.20 and δ 7.57 which we assigned to the 10,11-double bond. The lower-field doublet at δ 7.57 was tentatively assigned to the proton at the 11-position on the basis of its closer proximity to the electronegative oxygen on the quinone ring. It should be noted that a number of reaction conditions based on literature examples of the use of Fremy's salt[27] were investigated with the aim of minimizing the formation of side products in this somewhat capricious oxidation. The pH should optimally be maintained between 7.2 and 8.3, as the yield drops when the pH is <7.2, whereas a large amount of tar forms when the pH is >8.5. It is also important to continuously purge the system with argon during rotary evaporation of the reaction mixture to dryness. And finally, because **14** is somewhat unstable when adsorbed on silica gel, as well as air- and light-sensitive, it should not be allowed to remain on the column any longer than is necessary to obtain it in a pure enough state for the next step, and should be protected from bright illumination as much as possible.

Extraction of a solution of **14** in $CHCl_3$ in a separatory funnel with aqueous $Na_2S_2O_4$ (sodium hydrosulfite) for a few minutes until the color changed from red to yellow afforded the alcohol **l5** (87%) as a pale greenish-yellow solid whose ^{1}H NMR spectrum featured a pair of doublets at δ 6.07 and δ 6.17 for the azepinyl protons, a broad singlet at δ 6.04 for the proton on N-5, and a sharp singlet at δ 8.82 for the phenolic proton. The distinctive upfield shifts of the azepinyl protons, the C-1, C-3, and C-4 protons, and even the protons of the other ring in comparison with **14** were fully consistent with reduction of the quinone to a phenol. Treatment of **15** with *tert*-butylchlorodimethylsilane (TBDMSCl) and Et_3N in $CHCl_3$ (room temperature, 4 h) afforded the protected ether **16** (71%). This selective O-silylation step was critical in that it prevented reoxidation and also made it possible to selectively alkylate N-5 without O-alkylating the phenol.

Initial attempts to condense **16** with 2,4-diamino-6-bromomethylpteridine as in our earlier synthesis of **6** were unpromising, and we therefore turned our attention to the versatile synthon 2-amino-3-cyano-5-chloromethylpyrazine (**17**),[28] with which we already had some experience in the synthesis of 2,4-diamino-6-arylaminomethylpteridines with bulky aryl substituents.[29] When **16** and **17** were stirred in the presence of K_2CO_3 in MeCN at room temperature for 72 h the desired amino nitrile **18** was isolated in 43% yield as a light-yellow powder after silica gel flash chromatography (4:1 $CHCl_3$−MeOH). Notably, all the protons of the dibenzazepine ring system in **18** were shifted upfield relative to **15** and **16**, suggesting that the N-5 substituent has a pronounced effect on the magnetic ring current of the entire tricyclic system.

Although we had originally thought that heating **18** with guanidine in refluxing EtOH would result in ring closure without loss of the *O*-TBDMS group, we were pleasantly surprised to find that under the conditions used for this reaction (refluxing EtOH, 24 h) the protecting group was removed, presumably by the NaOEt used to convert guanidine hydrochloride to the free base. After chromatography on silica gel (85:15 $CHCl_3$−MeOH), the deprotected ring closure product **7** was obtained in 60% yield as a light-yellow powder. That the desired annulation product had formed with concomitant loss of the O-protecting group was confirmed by the ^{1}H NMR spectrum, which contained a singlet at δ 8.66, which is characteristic for the C-7 proton in 6-substituted 2,4-diaminopteridines, but no trace of a singlet at ca. δ 0.1 for the TBDMS group, which had been prominently visible in the spectra of **16** and **18**.

O-Alkylation of **7** was typically performed (except in one case as discussed below) in a one-pot operation in which freshly prepared NaOEt was dissolved in dry DMSO under an argon atmosphere, the phenol was then added, and after 30 min to allow the Na salt to form, a 10% molar excess of a bromo ester was added. The reaction mixture was left to stir overnight under argon, the ester group was cleaved directly with aqueous NaOH, and the deprotected product was isolated in analytically pure form by two-stage chromatography, initially on Dowex 50W−X2 (H_2O, then 1.5% NH_4OH to elute the product as an ammonium salt) and then on silica gel (3% AcOH in 4:1 $CHCl_3$−MeOH to elute the product as the free acid). In the case of the 2′-*O*-(2-carboxyethyl) analogue **9**, attempted alkylation of the anion of **7** with ethyl 3-bromopropanoate led to almost none of the desired ester, presumably reflecting facile base-catalyzed β-elimination to methyl acrylate. To circumvent this problem, alkylation of the anion of **7**

Table 1. Inhibition of *P. carinii, T, gondii, M. avium*, and Rat Liver DHFR by *N*-[(2,4-Diaminopteridin-6-yl)methyl]dibenz[*b,f*]azepine Derivatives

	IC_{50} (nM)[a]				selectivity index (SI)[b]		
compd	*P. carinii*	*T. gondii*	*M. avium*	rat liver	*P. carinii*	*T. gondii*	*M. avium*
6[c]	79 (58−110)	39 (32−47)	12 (9.1−17)	3000 (2500−3600)	38 (23−62)	77 (53−113)	250 (150−400)
7	31 (28−35)	26 (23−30)	1.3 (1.2−1.4)	41 (370−440)	13 (11−16)	16 (12−19)	320 (260−370)
8	21 (18−25)	17 (12−24)	8.2 (6.2−11)	280 (250−300)	13 (10−17)	16 (10−25)	34 (23−48)
9	24 (19−29)	28 (25−30)	4.0 (3.6−4.4)	1100 (1100−1200)	46 (12−63)	39 (37−48)	280 (250−330)
10	1.1[d] (0.92−1.3)	9.9 (8.9−11)	2.0 (1.7−2.3)	1500[d] (1100−1800)	1300 (850−2000)[d]	120 (90−160)	600 (430−820)
11	11 (9.8−12)	21(20−23)	7.2 (6.5−8.0)	1300 (1100−1500)	120 (80−150)	62 (55−65)	180 (140−230)
12	1.0[e] (0.88−1.2)	22 (18−27)	0.75 (0.55−1.0)	580[e] (500−680)	560 (420−780)[e]	26 (13−36)	630 (350−1200)
TMP[f]	13000 (10000−16000)	2800 (2400−3300)	300 (260−350)	180000 (160000−210000)	14 (10−20)	65 (48−87)	610 (460−810)
PTX[g]	13 (9.0−17)	4.3 (4.0−4.6)	0.61 (0.53−0.70)	3.3 (2.9−3.9)	0.26 (0.17−0.42)	0.76 (0.63−0.97)	5.4 (4.1−7.2)
TMX[h]	47 (34−66)	16 (8−30)	1.5 (1.3−1.7)	8.0 (7.0−9.2)	0.17 (0.11−0.27)	0.50 (0.23−1.2)	5.3 (3.4−7.2)

[a] Numbers in parentheses are 95% confidence intervals, rounded off to two significant figures and based on IC_{50} values likewise rounded off to two significant figures. The difference in IC_{50} between rat liver DHFR and each of the parasite enzymes was determined to be statistically significant at $P < 0.01$ (Welch's *t*-test). [b] SI = IC_{50}(rat liver DHFR)/IC_{50}(Pc, Tg, or Ma DHFR). Numbers in parentheses are 95% confidence intervals rounded off to two figures and represent a range calculated by dividing the lower end of the 95% confidence interval for the IC_{50} against rat liver DHFR by the upper end of the 95% confidence interval for the IC_{50} against Pc, Tg, or Ma DHFR; SI values of <1.0 signify lack of selectivity. [c] In our preliminary report on **6** (see ref 22), the IC_{50} values against Pc, Tg, Ma, and rat liver DHFR were listed as 210, 43, 12, and 4400 nM, respectively (with no 95% confidence limits provided). [d] In a separate experiment on a different day, the IC_{50} (nM) and SI values of **10** against Pc DHFR, with 95% confidence intervals in parentheses, were Pc, 1.1 (0.99−1.2), and 1100 (830−1200). [e] In a separate experiment on a different day, the IC_{50} (nM) and SI values of **12**, with 95% confidence intervals in parentheses), were 1.1 (0.90−1.0) and 430 (320−710). [f] TMP = trimethoprim, 2,4-diamino-5-(3′,4′,5′-trimethoxybenzyl)pyrimidine; data from ref 11b. [g] PTX = piritrexim, 2,4-diamino-5-methyl-6-(2′,5′-dimethoxybenzyl)pyrido[2,3-*d*]pyrimidine; data from ref 11b. [h] TMX = trimetrexate, 2,4-diamino-5-methyl-6-(3′,4′,5′-trimethoxyanilinomethyl)quinazoline.

was performed with 3-bromopropanoic acid in the presence of an extra 1 equiv of base. The superiority of 3-bromopropanoic acid over methyl 3-bromopropanoate in the O-alkylation of a phenolic OH group is well-known, and was noted, for example, by Kuyper and coworkers[30] during their synthesis of the trimethoprim analogue 2,4-diamino-5-[3′-*O*-(3-carboxyethoxy)-4′,5′-dimethoxybenzyl]pyrimidine. Interestingly, when the crude acid **9** was eluted from a Dowex 50W−X2 (H^+ form) column with 1.5% NH_4OH, and the eluate was acidified with HCl (instead of AcOH), freeze-dried, and finally chromatographed on silica gel using $CHCl_3$−MeOH as the eluent, the isolated product gave a TLC spot with a much higher R_f than would be expected from an acid, and its elemental analysis as well as ^1H NMR and mass spectra confirmed that it was in fact the *methyl ester* **9a**. Saponification of **9a**, followed by ion-exchange chromatography and acidification of the NH_4-OH eluate with HCl, yielded the hydrated sesquihydrochloride salt of **9** with an overall 22% yield starting from **7**.

Enzyme Inhibition

The ability of **8**−**12** and their phenolic precursor **7** to inhibit reduction of dihydrofolate by Pc, Tg, Ma, and rat DHFR in the presence of NADPH was determined spectrophotometrically at 340 nm according to the standardized assays we have used previously.[22,31,32] Compound **9** was tested as a sesquihydrochloride salt, the form in which it was obtained after purification, but this was not expected to affect the results since the pH of the DHFR assay medium was buffered to pH 7.4. The IC_{50} value and selectivity index (SI), together with the corresponding 95% confidence intervals, are shown for each compound in Table 1. Also included for comparison are the IC_{50} and SI values for trimethoprim and piritrexim as prototypical examples of DHFR inhibitors that can be viewed as weak but selective (trimethoprim) versus potent but nonselective (piritrexim).

***Pneumocystis carinii* DHFR.** The IC_{50} of the 2′-hydroxy derivative **7** against Pc DHFR was approximately 2-fold lower than that of **6**. However, because potency against rat DHFR increased to an even greater degree, this modification was unfavorable for selectivity against the Pc enzyme. Replacement of the 2′-hydroxy group by a 2′-*O*-carboxymethyl or 2′-*O*-(2-carboxyethyl) group as in **8** and **9**, respectively, did not improve inhibition of Pc DHFR in comparison with **7**. In contrast, the 2′-*O*-(3-carboxypropyl analogue **10** had an IC_{50} of 1.1 nM against Pc DHFR as compared with 1500 nM against the rat enzyme, corresponding to a selectivity index of 1300, a value 34 times greater than that of **6**, and among the highest we have observed in our work on Pc DHFR inhibitors to date. Interestingly, the longer homologue **11**, with four CH_2 groups in the side chain, was less potent and also less selective than **10**, indicating that potency and selectivity diminish when the number of CH_2 groups in the side chain exceeds three. This contrasted with our earlier findings on 2,4-diamino-[2′-methoxy-5′-(ω-carboxyalkyloxy)benzyl]pyrimidines, where potency and selectivity against Pc DHFR was greater with four rather than three CH_2 groups in the side chain.[11a] This difference can probably be explained on the basis that the larger diaminoheterocyclic moiety in **7** projects the COOH group somewhat differently into the binding pocket of the enzyme. Of interest, finally, was the considerable potency and selectivity of the 2′-*O*-(4-carboxybenzyl) analogue **12**, whose IC_{50} of 1.0 nM equaled that of **10** although its selectivity index of 560 was somewhat lower. This finding suggests that replacement of the $CH_2CH_2CH_2$ chain by a benzyl group is allowed, and that this type of structural modification may be worth exploring (e.g., by making the corresponding phenethyl derivative or moving the carboxyl group to the meta or ortho position).

Trimethoprim has been reported by workers at Hoffman-LaRoche to inhibit Pc and human DHFR with IC_{50} values of 46 and 900 μM, respectively, corresponding to a selectivity index of 20.[33] By contrast, in comparisons of the activity of trimethoprim against Pc and rat DHFR under standardized conditions, the average SI value observed by one of us (S.F.Q.) over a period of ap-

proximately 10 years has been only 14 (95% confidence interval 10−20) (Table 1). In assays comparing Pc and human DHFR the IC_{50} and selectivity values of the newer trimethoprim analogue 2,4-diamino-6-(3′,5′-diethoxy-4′-pyrrolobenzyl)pyrimidine (epiroprim, **19**) were

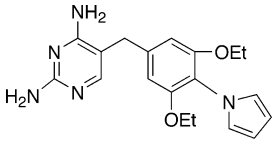

19 (epiroprim)

reported by the Hoffman-LaRoche group to be 3000 nM and 200, respectively,[33] whereas in assays comparing Pc and rat DHFR these values were found to be 2600 nM and 160.[34] Thus, the potency and selectivity **10** as an inhibitor of Pc DHFR appear to be superior to those of both trimethoprim and epiroprim.

Interestingly, when the selectivities of several antifolates, including **6** and trimethoprim, for Pc versus either rat or human DHFR were compared, a considerable variation in the species selectivity pattern was observed.[35,36] While the SI of trimethoprim for Pc versus human DHFR was ca. 50% higher than the SI for Pc versus rat DHFR, the SI of **6** for Pc versus rat and human enzyme was virtually the same. In striking contrast, the SI of the triazenyl pyrimethamine analogue TAB (**20**)[14a,b] for Pc versus human DHFR was 350-fold higher than the SI for Pc versus rat DHFR.

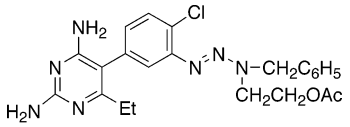

20 (TAB)

***Toxoplasma gondii* DHFR.** The 2′-hydroxy analogue **7** was nearly as potent as **6** against Tg DHFR, but was a 73-fold better inhibitor of the rat enzyme. As a result, **7** was less selective than **6**. The 2′-*O*-carboxymethyl analogue **8** was very similar to **7** in terms of both potency and selectivity. In the case of the 2′-*O*-(2-carboxyethyl) and 2′-*O*-(4-carboxybutyl) analogues **9** and **11** there was a small improvement in selectivity, but this reflected a decrease in the inhibition of the rat enzyme rather than an increase in inhibition of the Tg enzyme. On the other hand, the selectivity of 2′-*O*-(3-carboxypropyl) analogue **10** was clearly better than that of the other congeners, apparently as a result of the combined effect of increased inhibition of Tg DHFR and decreased inhibition of rat DHFR. Although **10** was the most potent and selective inhibitor of Tg DHFR among the compounds in this group, its selectivity was 10 times lower against this enzyme than against Pc DHFR, indicating that whatever differences in the 3D structure of the active site may exist between rat and Tg DHFR, these differences are not exploited as effectively by this 2′-modification as the corresponding differences between the rat and Pc enzymes.

In assays comparing Tg and human DHFR, the Hoffman-LaRoche group found trimethoprim to have IC_{50} values of 2700 nM and 900 000 nM, i.e., a selectivity index of 330.[33] For epiroprim (**19**), these values were 900 and 600 000 (i.e., a somewhat higher selectivity index of 670). More recently, Piper and co-workers[13a] reported a pteridine derivative, **21**, with IC_{50} values of 770 nM against Tg DHFR and 250 000 nM against rat DHFR (SI = 320), and a pyrido[2,3-*d*]pyrimidine derivative, **22**, whose corresponding IC_{50} values were 7.9 and 770 nM (SI = 98) Thus, **22** was more potent but less selective than **21**. Compound **10** (IC_{50} = 9.9 nM) was 78-fold more potent than **21** but only 7-fold more potent than **22**, and its selectivity index appeared to fall between the two of them. However, because 95% confidence intervals were not reported for **21** and **22**, the differences in selectivity among the three compounds should probably be viewed with caution. Regardless of whether the selectivity difference between **10** and **21** withstands statistical analysis, it seems clear that **10** is one of the most potent lipophilic 2,4-diamino-6-substituted pteridines we have encountered until now.

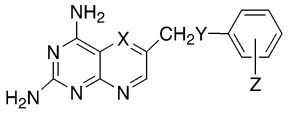

21 : X = N, Y = S, Z = SC_6H_5
22 : X = CMe, Y = CH_2, Z = 2,5-$(OMe)_2$

***Mycobacterium avium* DHFR.** As shown in Table 1, the 2′-hydroxy group in **7** resulted in a one-log increase in potency against *M. avium* DHFR relative to **6**, but because this was nearly matched by a 73-fold increase in potency against the rat enzyme, the selectivity index did not change appreciably. With the introduction of a 2′-*O*-(carboxymethyl) group, as in **8**, there was a slight increase in potency against Ma DHFR relative to **6**. However, because this was accompanied by a larger 11-fold *decrease* in potency against the rat enzyme, this modification appeared to have a detrimental effect on selectivity, just as it did in the case of the Pc and Tg enzymes. The 2′-*O*-(2-carboxyethyl) analogue **9** was 8-fold more selective than **8**, and this appeared to be due to a combination of increased inhibition of the Ma enzyme and decreased inhibition of the rat enzyme. Elongation of the side chain to three CH_2 groups, as in **10**, elicited a 4-fold increase in potency and an 18-fold increase in selectivity relative to **8**. However, when one more CH_2 group was introduced, as in **11**, potency and selectivity both decreased, recalling the pattern observed with **11** versus **10** against Pc and Tg DHFR. Replacement of the 2′-*O*-(3-carboxypropyl) group of **10** by a 2′-*O*-(4-carboxybenzyl) group, as in **12**, led to a modest increase in potency against the Ma enzyme, but because this was accompanied by a similar increase in potency against the rat enzyme there was essentially no change in selectivity, with both compounds giving an SI value of ca. 600. The IC_{50} of **12** against Ma DHFR was several times lower than the reported values for 2,4-diamino-5-[2′-methoxy-5′-*O*-(4-carboxybutyl)oxybenzyl]pyrimidine (**23**, IC_{50} = 5.8 nM)[11a] and 2,4-diamino-5-[2′-methoxy-5′-(4-carboxy-1-butynyl)benzyl]pyrimidine (**24**, IC_{50} = 4.4 nM),[11b] the most potent inhibitors of this enzyme we had encountered up to that point. Apart from its excellent potency, the selectivity of **12** for Ma versus rat DHFR (SI = 630) was of the same order as that of **23** (SI = 660) and **24** (SI = 910). It should be noted, however, that **10** and **12** are neither

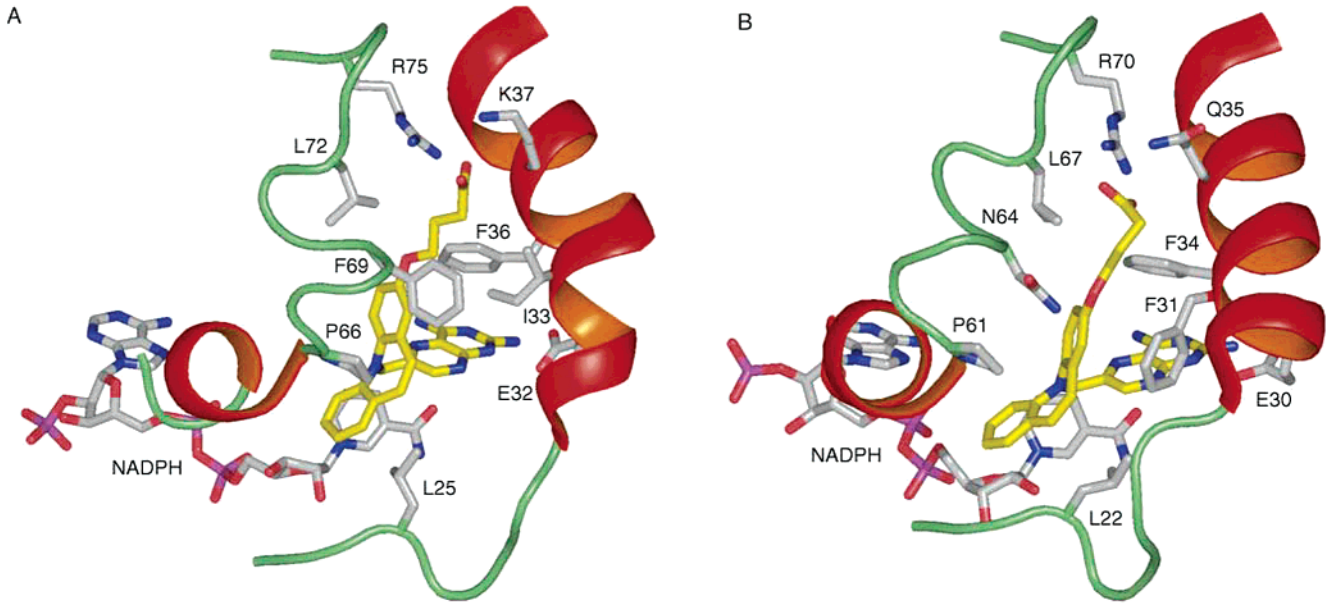

Figure 1. Structures of the ternary complexes of **10** and NADPH with *P. carinii* (Panel A) and human (Panel B) DHFR after 0.5 ns dynamic simulation. Model produced using the PYMOL Molecular Graphics System (DeLano Scientific, San Carlos, CA). Hydrogen atoms are omitted for clarity.

the most potent nor the most selective Ma DHFR inhibitors thus far described in the literature. For example, workers at Hoffman-LaRoche have reported that epiroprim (**19**) has an IC_{50} of 4.1 nM against Ma DHFR and a prodigious selectivity index of >14 000 relative to the human enzyme.[33] A second compound, 2,4-diamino-5-methyl-6-[(3′,5′-di-*n*-propyloxyanilino)-methyl]pyrido[2,3-*d*]pyrimidine (**25**), which may be viewed as an analogue of both piritrexim (heterocyclic system) and trimetrexate (bridge), was reported by Suling and co-workers[13b] to have an IC_{50} of only 0.19 nM against Ma DHFR, with a selectivity index of 7300 relative to the human enzyme. Several other compounds in their series had IC_{50} values of <1.0 nM and selectivities of >1000.[37] Since the SI of **6** for Pc versus human DHFR has been found to be comparable to its SI for Pc versus rat DHFR,[35] and compounds **10** and **12** have the same basic structure as **6**, their SI for Ma versus human DHFR is not likely to differ much from the values in Table 1. Thus, where Ma DHFR inhibition is concerned, these compounds are of interest only insofar as they are the best *pteridine* derivatives in our work to date. However, on the basis of the results obtained by the Southern Research Institute groups,[13b] analogues of **25**

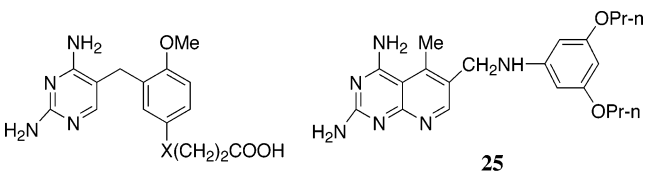

23: X = -C≡C-
24: X = OCH_2CH_2

25

with a 2′-(3-carboxypropyl)oxy moiety in the side chain would be of potential interest. Given the promising in vitro data recently reported for the combination epiroprim−dapsone against *Mycobacterium leprae* and *Mycobacterium ulcerans*,[38] potent and selective DHFR inhibitors of the type reported in this paper could be considered for testing against non-AIDS associated mycobacteria.

Modeling Studies

To better understand the reason for the remarkable selectivity of binding of **10** to Pc DHFR, we used Sybyl 6.9[39] on a Silicon Graphics Octane 2 workstation to perform a computational simulation of the 3D structure of the ternary complex with NADPH. The starting coordinates for the simulation were generated by least-squares superposition of the pteridine moiety of **10** onto the previously solved crystal structure of the ternary complex with Pc and human DHFR with **6** as the bound ligand.[22,23] The complex was solvated in a box of water, but the current force field did not take polarizable parameters into account. In considering such a model, it is important to remember that molecular dynamics can only regarded as snapshots of low energy states, and that a global minimum is unlikely to be derived by this method even after extensive cycles of dynamics simulation and energy minimization.

The simulated structure of the ternary complex of **10** and NADPH with Pc and human DHFR is presented in Figure 1, which depicts a view looking down into the cleft of the enzyme where the diaminopyrimidine moiety lies buried. Based on the finding that every residue in the active site of human and rat DHFR is conserved,[35] the assumption was made that the 3D structure of the ternary complex of **10** would probably be very similar, if not identical, with both enzymes. Visible in both Panel A and Panel B is the nonplanar dibenzazepine ring system and its rotationally twisted orientation with respect to the diaminopteridine moiety, already noted in the case of **6**.[23] Important active site residues located within a 4.5 Å radius from the inhibitor are denoted according to standard amino acid nomenclature. The inhibitor is anchored to both enzymes through the usual interaction of protonated N1 and the 2-amino group of the pteridine moiety with glutamic acid (E32 in the Pc enzyme; E30 in the human enzyme). The N4 amino group lies within H-bonding distance of backbone amide oxygens in I10 and I123 of Pc DHFR and I7 and V115 of human DHFR (omitted from the figure). The inhibitor

lies in a hydrophobic channel that allows for van der Waals interaction of the dibenzazepine moiety with phenylalanine (F69, 5.75 Å to the center of the A-ring,[40] offset stacking), proline (P66, 3.77 Å from the center of the B-ring), and leucine (L25, 3.80 Å to the center of C-ring) in the case of the Pc enzyme, and with phenylalanine (F31, 4.65 Å to the center of the A-ring, offset stacking), and proline (P61, 4.14 Å to the center of the B-ring) in the case of the human enzyme. The offset stacking interaction of F69 with one face of the A-ring in the Pc enzyme is not possible in the human enzyme, whose corresponding residue is asparagine (N64). Instead there is in the human ternary complex an offset stacking interaction of F31 with the opposite face of the A-ring. Probably of greatest importance in terms of species-selective DHFR inhibition, however, is the ionic or H-bonded interaction of the terminal COOH group of **10** with the ϵ-amino group of a lysine residue (K37) in Pc DHFR, which is not possible in the case of the human enzyme because the homologous residue is a neutral glutamine (Q35). Although it would possible in principle for the $CONH_2$ side chain of Q35 to engage in an ion−dipole interaction with this COOH group, the contribution of ion−dipole interactions in molecular recognition is considered to be weaker than ionic interactions.[41] Thus ion−dipole interaction between the COOH group and Q35 in human DHFR is unlikely to produce as much binding energy as ionic interaction of the COOH group with the positively charged amino group of K37 in Pc DHFR.

The COOH group of **10** appears to lie within approximately 3 Å of the arginine side chain in both the Pc (R75) and the human (R70) enzyme. The energy-minimized distances between the O2 and O3 atoms of the COOH group and the ϵ-NH_2 group of K37 are 3.19 and 3.09 Å. The distances between these oxygens and the N2 and N1 atoms, respectively, of the guanidine group are 4.02 and 2.99 Å for Pc DHFR, and 2.96 and 2.97 Å for human DHFR. Since the arginine residue is conserved in both enzymes, it presumably cannot account for the observed preferential inhibition of the Pc enzyme. It is worth noting that similar interactions of the lysine and arginine residues in Pc and human DHFR with the side-chain COOH group of **24** were predicted from modeling studies[42a] and subsequently confirmed by crystallography.[42b] Crystallographic analysis of the 3D structure of the ternary complex of **10** with NADPH and Pc DHFR is currently being performed in Dr. Vivian Cody's laboratory, and the results will be reported in due course.

Conclusion

In summary, six 2,4-diamino-6-(dibenz[*b*,*f*]azepin-5-yl)methylpteridine analogues in which a 2′-(ω-carboxyalkyloxy) or a 2′-(4-carboxybenzyloxy) substituent has been introduced in order to afford water solubility and enhance DHFR affinity were synthesized and tested as inhibitors of Pc, Tg, Ma, and rat DHFR. 2,4-Diamino-6-[2′-*O*-(3′-carboxypropyl)oxydibenz[*b*,*f*]azepin-5-yl]methylpteridine (**10**) was an exceptionally potent and selective inhibitor of the Pc enzyme, with an IC_{50} of 1.1 nM and a selectivity of 1300 for the Pc enzyme versus the rat enzyme (IC_{50} = 1500 nM). This compound was likewise a good inhibitor of Tg and Ma DHFR, with IC_{50} values of 9.9 and 2.0 nM and SI values of 120 and 600, respectively. Thus it was somewhat less potent and selective against these enzymes than against Pc DHFR. 2,4-Diamino-6-[2′-*O*-(4-carboxybenzyl)oxydibenz[*b*,*f*]azepine (**12**) was as potent as **10** but somewhat less selective against Pc and Tg DHFR and was approximately as potent and selective against Ma DHFR. These compounds are the most active pteridines we have tested to date against these enzymes and may be viewed as promising leads for further investigation. Especially attractive would be the possibility of using a compound such as **10** without coadministration of a sulfa drug to boost efficacy or leucovorin to prevent host toxicity.

Experimental Section

IR spectra in KBr disks were obtained on a Perkin-Elmer Model 781 double-beam recording spectrophotometer; only peaks with wavenumbers greater than 1200 cm^{-1} are reported. ^1H NMR spectra were recorded in DMSO-d_6 solution at 200 MHz on a Varian VX200 instrument or at 400 MHz on a Varian VX400 instrument. Quantitative UV spectra were determined in 4:1 MeCN−H_2O ($c = 5 \times 10^{-4}$ M) on a Perkin-Elmer 35 UV/visible instrument. Low-resolution MS data were provided by the Molecular Biology Core Facility of the Dana-Farber Cancer Institute. TLC was on Whatman MK6F silica gel-coated microscope slides, with spots being visualized under 254 nm UV illumination. Preparative TLC was on silica gel-coated glass plates (Aldrich, 1000 μm layer, 20 × 20 cm, with fluorescent indicator). Column chromatography was on silica gel ('Flash' grade, Baker 7024, 40 μm particle size). Chemicals and 'Sure-Seal' solvents were purchased from Aldrich (Milwaukee, WI). Melting points were determined in Pyrex capillary tubes in a Mel-Temp apparatus (Laboratory Devices, Inc., Cambridge, MA) and are not corrected. Elemental analyses were performed by QTI Laboratories, Whitehouse, NJ, or Robertson Laboratories, Madison, NJ, and were within ±0.4 of theoretical values unless otherwise noted. As has been our previous experience with *N*-heterocyclic compounds of the type synthesized in this work, the analytical data were consistent with varying amounts of residual AcOH, MeOH, $CHCl_3$, or H_2O in the analytical samples, which were dried in vacuo, but only at the ambient temperature of the laboratory. The presence of residual solvent was confirmed wherever possible by ^1H NMR. Although chlorine analysis was not performed on compounds **8** and **12**, their assigned elemental composition was supported in both cases by the presence of the correct molecular ion (MH^+) in the mass spectrum.

Dibenz[*b*,*f*]azepin-2-one (14). A solution $(KSO_3)_2NO$ (Fremy's salt, 2.5 g, 9.32 mmol) was added in small portions to a solution of Na_2HPO_2 (1.8 g, 12.7 mmol) in double-distilled H_2O (95 mL), and the pH was adjusted to exactly 7.22 with a meter. Small portions of the purple solution were then added to a vigorously stirred solution of **13** (0.55 g, 2.76 mmol) in acetone (60 mL), and after 10 min the mixture was filtered and left in the refrigerator overnight. After concentration to a small volume by rotary evaporation under a stream of argon (while keeping the water bath at room temperature for best results), the product was extracted into Et_2O (500 mL). The solvent was evaporated and the residue chromatographed on silica gel using a 4:1 mixture of hexanes and EtOAc as the eluent. The first fraction was unchanged **13** which could be pooled from several experiments and recycled (56 mg, ca. 10% recovery). The second fraction, a yellow solid, was determined to be acridine-9-carboxaldehyde (70 mg); ^1H NMR ($CDCl_3$) δ 11.5 (CH=O). The third fraction, a deep-red microcrystalline powder after recrystallization from Et_2O, was the desired iminoquinone **14** (0.44 g, 77%); mp 133−134 °C (lit.,[25] 135−136 °C); ^1H NMR: δ 6.69 (d, J = 2.4 Hz, 1H, H1), 6.95 (dd, J = 12.8 Hz, J = 2.4 Hz, 1H, H3), 7.01 (d, J = 12.8 Hz, 1H, H4), 7.20 (d, J = 11.8 Hz, 1H, H11), 7.57 (d, J = 11.8 Hz, 1H, H10), 7.65−7.92 (complex m, 4H, H6−H9).

2-Hydroxy-5*H*-dibenz[*b,f*]azepine (15). A solution of **14** (0.3 g, 1.45 mmol) in $CHCl_3$ (10 mL) was shaken in a separatory funnel with freshly prepared solution containing an excess of $Na_2S_2O_4$ (0.62 g, 3.56 mmol) in H_2O (4 mL) until the color of the organic layer changed from red to yellow. The aqueous layer was extracted with $CHCl_3$ (2 × 10 mL), the combined organic extracts were dried (Na_2SO_4), and the solvent was evaporated by rotary distillation. Recrystallization of the residue from $CHCl_3$ afforded **15** as pale greenish-yellow crystals (0.26 g, 87%); mp 222−223 °C (lit.[26] 225−226 °C); ^{1}H NMR: δ 6.04 (br s, NH), 6.07 (d, J = 11.8 Hz, 1H, H10 or H11), 6.16 (d, J = 11.8 Hz, 1H, H10 or H11), 6.23 (d, J = 2.2 Hz, 1H, H1), 6.40 (d, J = 8.6 Hz, J = 2.2 Hz, 1H, H3), 6.48 (d, J = 8.6 Hz,1H, H4), 6.59−6.70 (complex m, 4H, H6−H9), 8.82 (s, 1H, phenolic OH).

2-(*tert*-Butyldimethylsilyloxy)-5*H*-dibenz[*b,f*]azepine (16). A mixture of **15** (1.4 g, 6.7 mmol), *tert*-butylchlorodimethylsilane (2.5 g, 19 mmol), and Et_3N (1 mL) in dry $CHCl_3$ (80 mL) was stirred at room temperature for 48 h. The solvent and excess silane were removed by rotary evaporation, and the residue was chromatographed on silica gel with a 4:1 mixture of hexanes and EtOAc to obtain **14** as a yellow solid (1.55 g, 71%); mp 188−189 °C; ^{1}H NMR: δ 0.13 (6H, $SiMe_2$, 0.92 (s, 9H, SiBu-t), 6.06 (broad s, NH), 6.08 (d, J = 12.2 Hz, 1H, H10 or H11), 6.10 (d, J = 12.2 Hz, 1H, H10 or H11), 6.29 (d, J = 2.2 Hz, 1H, H1), 6.50 (q, J = 8.0 Hz, 1H, H3), 6.58 (d, J = 8.0 Hz, 1H, H4), 6.63−6.96 (complex m, 4H, H6−H9). Anal. ($C_{20}H_{25}NOSi$) C, H, N; Si, calcd 8.68, found 9.27.

2-Amino-3-cyano-5-[2′-(*tert*-butyldimethylsilyl)oxydibenz[*b,f*]azepin-5-yl]pyrazine (18). A suspension of **16** (1.62 g, 5 mmol) in anhydrous MeCN (50 mL) was treated with **17** (0.85 g, 5 mmol) and powdered K_2CO_3 (1.4 g, 10 mmol), and the reaction mixture was stirred at room temperature for 72 h. The salts were filtered off, the filter cake was extracted with hot EtOAc, and the combined organic solvents were removed by rotary evaporation. Flash chromatography of the amber-colored residue on silica gel using a 4:1 mixture of $CHCl_3$ and MeOH as the eluent afforded **15** as a light-yellow powder (0.95 g, 43%) mp 204−205 °C; ^{1}H NMR: δ 0.11 (s, 6H, $SiMe_2$), 0.89 (s, 9H, SiBu-t), 4.85 (s, 1H, NCH_2), 6.60 (br s, NH), 6.72 (d, J = 8.6 Hz, 1H, H3′), 6.78 (s, 1H, H1′), 6.83 (d, J = 8.6 Hz, 1H, H4′), 6.95 (d. J = 8.4 Hz, 1H, H10′ or H11′), 6.98 (d, J = 8.4 Hz, 1H, H10′ or H11′), 7.13−7.78 (complex m, 4H, H6′−H9′), 7.43 (br s, NH_2), 8.20 (s, 1H, pyrazine H6).

2,4-Diamino-6-(2′-hydroxydibenz[*b,f*]azepin-5-yl)methylpteridine (7). Clean Na metal (0.12 g, 5 mmol) was dissolved in absolute EtOH (30 mL), and guanidine hydrochloride (0.48 g, 5 mmol) was added in a single portion. After 5 min of stirring at room temperature, amino nitrile **18** (0.82 g, 1.8 mmol) was added and the mixture was refluxed for 24 h. The solvent was removed by rotary evaporation, and the residue was triturated with H_2O (20 mL) and filtered. The product was dissolved in MeOH (20 mL) and the solution evaporated onto silica gel (1 g). The dried silica gel was placed on top of a silica gel column which was eluted 85:15 $CHCl_3$−MeOH to obtain **7** as a yellow solid (0.44 g, 60%); mp 251 °C dec; MS: found *m/e* 384.1, calcd 384.2 (MH^+); IR: ν 3460, 3400, 1620, 1450, 1360, 1210 cm^{-1}; UV: λ_{max} 373 nm (ϵ 8277); ^{1}H NMR: δ 5.03 (s, 2H, NCH_2), 6.51 (d, J = 2.0 Hz, 1H, H1′), 6.62 (q, J = 8.8 Hz, J = 2.0 Hz, 1H, H3′), 6.79 (d, J = 11.4 Hz, 1H, H10′ or H11′), 6.83 (d, J = 11.4 Hz, 1H, H10′ or H11′), 6.97 (d, J = 8.8 Hz, 1H, H4′), 7.11−7.23 (complex m, 4H, H6′−H9′), 7.49 (br s, NH_2), 7.60 (br s, 1H, NH_2), 8.66 (s, 1H, pteridine H7), 9.18 (br s,1H, phenolic OH). Anal. ($C_{21}H_{17}N_7O\cdot 0.7H_2O$) C, H, N.

2,4-Diamino-6-[2′-(ω-carboxyalkyl)oxy- or 2′-(4-carboxybenzyl)oxydibenz[*b,f*]azepin-6-yl]methylpteridines (General Procedure). Clean metallic Na (12 mg, 0.5 mmol) was dissolved in absolute EtOH (1 mL), the solvent was evaporated under reduced pressure, and the NaOEt was redissolved in anhydrous DMSO (1.5 mL). The phenol **7** (190 mg, 0.5 mmol) was then added, the reaction mixture containing the Na salt of **7** was stirred at room temperature for 30 min, the appropriate bromo ester (0.6 mmol) was added in a single portion, and the flask was fitted with a balloon of dry argon. TLC (silica gel, 4:1 $CHCl_3$−MeOH) easily revealed gradual loss of the spot corresponding to the starting material and its replacement by a faster-moving spot. The reaction was allowed to proceed overnight under argon, and the product was immediately saponified in situ by adding 2 N NaOH (1.5 mL) followed by H_2O to a final volume of 60 mL. Any insoluble material remaining at this point was filtered off, and after addition of a small volume of dilute ammonia, the clear solution was applied onto a column of Dowex 50W−X2 (H^+ form, 2 cm × 20 cm). The column was washed with H_2O until the eluate was neutral and UV-transparent, and then with 1.5% NH_4-OH to remove the product as a mixture of sodium and ammonium salts. Appropriately pooled eluates were concentrated to a small volume (or to dryness) by rotary evaporation followed by lyophilization. The solid was taken up in the minimum volume of MeOH required to dissolve it, silica gel (0.5 g) was added, and the mixture was taken to dryness by rotary evaporation. The silica gel with preadsorbed product was loaded onto a silica gel column packed in $CHCl_3$, and the product was eluted with 3% AcOH in 4:1 $CHCl_3$−MeOH. Purification was monitored by TLC, and appropriately pooled fractions containing the product were evaporated and dried in vacuo in a lyophilization apparatus. Compounds **8**, **10**, and **11** were obtained in this procedure, whereas **9** was prepared by a slight variation of the method detailed below.

2,4-Diamino-6-[2′-*O*-(carboxymethyl)oxydibenz[*b,f*]-azepin-5-yl]methylpteridine (8): tan solid (101 mg, 35%); mp 223 °C dec; MS: found *m/e* 441.9, calcd 442.2 (MH^+); IR: ν 3420, 3200, 1700, 1630, 1500, 1480, 1450, 1380, 1220, 1070 cm^{-1}; UV: λ_{max} 353 nm (ϵ 5785); ^{1}H NMR: δ 4.51 (s 2H, CH_2O), 5.06 (s, 2H, CH_2N), 6.57 (br s, NH_2), 6.69 (d, J = 2.8 Hz, 1H, H1′), 6.79 (q, J = 8.9 Hz, J = 2.8 Hz, H3′), 6.83 (d, J = 6.2 Hz, 1H, H10′ or H11′), 6.84 (d, J = 6.2 Hz, 1H, H10′ or H11′), 6.90 (d, J = 8.9 Hz, 1H, H4′), 6.90−7.24 (m, complex m, H6′−H9′), 7.52 (br s, NH_2), 8.67 (s, 1H, pteridine H_7), 12.22 (br s, COOH). Anal. ($C_{23}H_{19}N_7O_3\cdot$ MeOH·0.4$CHCl_3$) C, H, N.

2,4-Diamino-6-[2′-*O*-(2-carboxyethyl)oxydibenz[*b,f*]-azepin-5-yl]methylpteridine (9). Clean metallic Na (24 mg, 1.0 mmol) was dissolved in absolute EtOH (2 mL), the solvent was evaporated under reduced pressure, and the residue was taken up in dry DMSO (1.5 mL). The phenol **7** (190 mg, 0.5 mmol) was then added, and the mixture was stirred at room temperature for 30 min, followed by addition of 3-bromopropanoic acid (79 mg, 0.5 mmol) in a single portion. After being stirred overnight under dry argon, the mixture was evaporated under reduced pressure and the residue was dissolved in H_2O (60 mL) and 2 N NaOH (1 mL). The clear solution was applied onto a column of Dowex 50W−X2 (H^+ form, 2 cm × 20 cm), and the column was washed with H_2O until the eluate was neutral and UV-transparent and then with 1.5% NH_4OH to elute the product. Appropriately pooled fractions of the latter eluate were acidified to pH 2 with 10% HCl, followed by rotary evaporation and freeze-drying. The resulting solid was taken up in MeOH (10 mL), chromatography-grade silica gel (0.5 g) was added to the solution, and the mixture was evaporated to dryness. The silica gel with preadsorbed product was then placed on a column of silica gel which had been prepacked with $CHCl_3$. The column was eluted with 4:1 $CHCl_3$−MeOH as in the preceding experiment, and the major band was collected and evaporated to a brown solid which proved to be the *methyl ester* of **9**; 88 mg, 38%); mp 240−241 °C dec; MS: found *m/e* 470.0, calcd 470.5 (MH^+); ^{1}H NMR: δ 2.72 (t, 2H, J = 6.2 Hz, CH_2COOH), 3.59 (s, 3H, OMe), 4.10 (t, 2H, J = 6.2 Hz, OCH_2), 5.07 (s, 2H, NCH_2), 6.63 (d, 1H, J = 7.0 Hz, H10′ or H11′), 6.74 (q, J = 8.9 Hz, J = 2.8 Hz, H3′), 6.85 (d, 1H, J = 7.0 Hz, H10′ or H11′), 6.98 (d, 1H, J = 8.9 Hz, H4′), 6.70−7.24 (complex m, 4H, H6′−H9′), 7.56 (br s, NH_2), 7.65 (br s, NH_2), 8.67 (s, 1H, pteridine H7). Anal. ($C_{25}H_{23}N_7O_3\cdot$MeOH). C,H,N.

Saponification of **9** was carried out by stirring it 2 N NaOH (1.5 mL) at room temperature while monitoring the reaction by TLC (silica gel, 85:15 $CHCl_3$−MeOH). A clear solution gradually formed, and the fast-moving ester spot was replaced by a slow-moving spot where the acid was expected to be. After

15 min, the solution was diluted with H_2O to a final volume of 40 mL and applied to the top of a Dowex 50W−X2 column (H^+ form, 2 cm, 20 cm). The column was eluted with H_2O until the eluate was neutral and then with 1.5% NH_4OH. Appropriately pooled fractions of the NH_4OH eluate were acidified to pH 1 with 10% HCl followed by the same the workup as above afforded a beige solid (51 mg, 22% based on **7**); mp 242 °C dec); MS: *m/e* 455.9, calcd 455.2 (MH^+, free acid); IR (KBr) ν 3420, 3200, 1615, 1550, 1480, 1450, 1380, 1360, 1285, 1200 cm^{-1}; UV: λ_{max} (H_2O) 350 nm (ϵ 7630); λ_{max} (MeCN) 383 nm (ϵ 7246); NMR: δ 2.64 (t, 2H, J = 6.0 Hz, CH_2COOH), 4.07 (t, 2H, OCH_2), 5.04 (s, 2H, NCH_2), 6.63 (d, 1H, J = 2.8 Hz, H1′), 6.74 (q, 1H, J = 8.9 Hz, J = 2.8 Hz, H3′), 6.79 (d, 1H, J = 7.0 Hz, H10′ or H11′), 6.80 (d, 1H, J = 7.0 Hz, H10′ or H11′), 6.95 (d, 1H, J = 8.9 Hz, H4′), 7.06−7.24 (m, 4H, H6′−H9′), 7.61 (br s, NH_2), 7.69 (br s, NH_2), 8.67 (s, 1H, pteridine H7), 12.31 (br s, COOH). Anal. ($C_{24}H_{21}N_7O_3 \cdot 1.5HCl \cdot H_2O$) C, H, N.

2,4-Diamino-6-[2′-*O*-(3-carboxypropyl)oxydibenz[*b,f*]-azepin-5-yl]methylpteridine (10): tan solid (157 mg, 58%); mp 236 °C dec; MS: found *m/e* 470.0, calcd 470.2 (MH^+); IR: ν 3440, 3400, 1700, 1630, 1550, 1450, 1380, 1200 cm^{-1}; UV: λ_{max} 363 nm (ϵ 5874); ^{1}H NMR: δ 1.86 (m, 2H, $CH_2CH_2CH_2$), 2.32 (t, J = 7.4 Hz, 2H, CH_2COOH), 3.87 (t, J = 6.4 Hz, 2H, OCH_2), 5.06 (s, 2H, NCH_2), 6.56 (br s, NH_2), 6.71 (d, J = 2.6 Hz, H1′), 6.77 (q, J = 8.8 Hz, J = 2.6 Hz, 1H, H3′), 6.84 (d, J = 6.2 Hz, 1H, H10′ or H11′), 6.85 (d, J = 6.2 Hz, 1H, H10′ or H11′), 7.01 (d, J = 8.8 Hz, 1H, H4′), 6.91−7.28 (complex m, 4H, H6′−H9′), 7.55 (br s, NH_2), 8.67 (s, 1H, pteridine H7), 12.01 (br s, COOH). Anal. ($C_{25}H_{23}N_7O_3 \cdot MeOH \cdot 0.9H_2O$) C, H, N.

2,4-Diamino-6-[2′-*O*-(4-carboxybutyl)oxydibenz[*b,f*]-azepin-5-yl]methylpteridine (11): tan solid (145 mg, 48%); mp 232 °C dec; IR: ν 3420, 3400, 1620, 1480, 1450, 1200 cm^{-1}; MS: found *m/e* 484.1, calcd 484.2 (MH^+); UV: λ_{max} 375 nm (ϵ 5694); ^{1}H NMR: δ 1.60 (m, 4H, OCH_2CH_2), 2.23 (t, J = 6.6 Hz, 2H, CH_2COOH), 3.84 (t, 2H, J = 6.0 Hz, OCH_2), 5.07 (s, 2H, NCH_2), 6.58 (br s, NH_2), 6.72 (d, J = 2.8 Hz, 1H, H1′), 6.77 (q, J = 8.8 Hz, J = 2.8 Hz, 1H, H3′), 6.83 (d, J = 6.2 Hz, 1H, H10′ or H11′), 6.84 (d, J = 6.2 Hz, 1H, H10′ or H11′), 7.01 (d, J = 8.8 Hz, 1H, H4′), 6.91−7.28 (complex m, 4H, H6′−H9′), 7.50 (br s, NH_2), 8.67 (s, 1H, pteridine H7), 12.00 (br, COOH). Anal. ($C_{26}H_{25}N_7O_3 \cdot 1.2AcOH \cdot 0.5 \cdot i\text{-}PrOH$) C, H, N.

2,4-Diamino-6-[2′-(4-carboxybenzyl)oxydibenz[*b,f*]-azepin-5-yl]methylpteridine (12): tan solid (95 mg, 32%); mp 244−245 °C; MS: found 518.0, calcd 518.2; UV: λ_{max} 368 nm (ϵ 5845); ^{1}H NMR: δ 5.09 (s, 2H, NCH_2), 6.57 (s, 2H, OCH_2), 6.84 (d, J = 7.4 Hz, 1H, H10′ or H11′), 6.88 (d, J = 7.4 Hz, 1H, H10′ or H11′), 6.91 (s, 1H, H1′), 7.00 (d, J = 7.6 Hz, 1H, H3′), 7.10 (d, J = 7.6 Hz, 1H, H4′), 7.17−7.24 (complex m, 4H, H6′−H9′), 7.49 (d, J = 8.0 Hz, 2H, protons *meta* to COOH), 7.51−7.89 (br s, NH_2), 7.91 (d, J = 8.0 Hz, 2H, protons *ortho* to COOH). 8.68 (s, 1H, pteridine H7), 12.29 (br s, COOH). Anal. ($C_{29}H_{23}N_7O_3 \cdot 0.9MeOH \cdot 0.4CHCl_3$) C, H; N, calcd 16.08, found 16.50.

Dihydrofolate Reductase Inhibition. IC_{50} values for inhibition of Pc and rat DHFR were obtained as described earlier.[22]

Molecular Modeling Studies (by D. Chan). Computational simulations were performed using the molecular dynamics package AMBER 7[43] implementing the all-atom nonpolarizable ff99 force field[44] based on the force field of Cornell and co-workers.[45] Molecular mechanics parameters for **10** and NADPH were not present in the standard AMBER database and thus were derived using ANTECHAMBER.[46] AM1-BCC partial charges were obtained from MOPAC.[47] Formal charges of −1 and −4 were assigned to **10** and NADPH, respectively. Starting coordinates for the simulations were furnished by least-squares superimposition of the pteridine moiety of **10** onto inhibitors displayed in previously reported ternary complexes of Pc DHFR (PDB code: 1KLK)[23] and human DHFR (PDB code: 1OHJ)[48] using the molecular graphics package Sybyl 6.9.[39] The carboxyalkoxy side chain of **10** was manually rotated to minimize steric clashes with the enzyme. All crystallographically determined H_2O molecules were retained except two, which were removed from the active site in order to accommodate the dibenz[*b,f*]azepine moiety. The ternary complexes were solvated in TIP3 H_2O by adding a 10 Å (Pc DHFR) or 9 Å (human DHFR) shell around the solute, raising the total number of H_2O molecules in the system to 7262 and 8106, respectively. All molecular dynamics simulations were unrestrained and began with a 2000-step energy minimization protocol consisting of cycles of steepest descent minimization, followed by conjugate gradient minimization to remove unfavorable contacts between the enzyme, NADPH, and **10**. Periodic boundary conditions with a nonbonded cutoff of 10 Å were applied. Dynamics runs were 0.5 ns in length and had a time step of 2 fs. The pressure was regulated at 1 atm, and the temperature was maintained at 298 K with the exception of the final 20 ps, when the system was cooled to 1 K over a period of 10 ps. The SHAKE algorithm[49] was applied to constrain bonds involving hydrogen at their equilibrium values. At the end, the complexes were subjected to a 2000-step energy minimization procedure.

Acknowledgment. This work was supported in part by Grant RO1-AI29904 (A.R.) from the National Institute of Allergy and Infectious Diseases. Computer time was generously provided by the Research Computing Core Facility, Dana-Farber Cancer Institute.

References

(1) Richman, D. D. HIV chemotherapy. *Nature* **2001**, *410*, 995−1001.
(2) Menéndez-Arias, L. Targeting HIV: antiretroviral therapy and development of drug resistance. *Trends Pharmacol. Sci.* **2002**, *23*, 381−388.
(3) (a) Moore, R. D. Cost-effectiveness of combination HIV therapy; 3 years later. *Pharmacoeconomics* **2000**, *17*, 325−330. (b) Freedberg, K. A.; Losina, E.; Weinstein, M. C.; Paltiel, A. D.; Cohen, C. J.; Seage, G. R.; Craven, D. E.; Zhang, H.; Kimmel, A. D.; Goldie, S. J. The cost-effectiveness of combination antiretroviral therapy for HIV disease. *N. Engl. J. Med.* **2001**, *344*, 824−831.
(4) (a) Kaplan, J. E.; Hu, D. J.; Holmes, K. K.; Jaffe, H. W.; Masur, H.; De Cock, K. M. Preventing opportunistic infections in human immunodeficiency virus-infected persons: implications for the developing world. *Am. J. Trop. Med. Hyg.* **1996**, *55*, 1−11. (b) Moore, R. D.; Chaisson, R. E. Natural history of opportunistic disease in an HIV-infected urban clinical cohort. *Ann. Intern. Med.* **1996**, *124*, 633−642.
(5) (a) Piot, P. Global AIDS epidemic: time to turn the tide. *Science* **2000**, *288*, 2176−2178. (b) Parker, R. The global HIV/AIDS pandemic, structural inequalities, and the politics of international health. *Am. J. Public Health* **2002**, *92*, 343−346.
(6) Kovacs, J. A.; Gill, V. J.; Meshnick, S.; Masur, H. New insights into transmission, diagnosis, and drug treatment of *Pneumocystis carinii* pneumonia. *J. Am. Med. Assoc.* **2001**, *286*, 2450−2460.
(7) Wong, S. Y.; Remington, J. S. Biology of *Toxoplasma gondii*. *AIDS* **1993**, *7*, 299−316.
(8) (a) Belanger, F.; Derouin, F.; Grangeot-Keros, L.; Meyer, L. Incidence and risk factors of toxoplasmosis in a cohort of human immunodeficiency virus-infected patients: 1988−1995. HEMOCO and SEROCO Study Groups. *Clin. Infect. Dis.* **1999**, *28*, 575−581. (b) Neuenburg, J. K.; Brodt, H. R.; Herndier, B. G.; Bickel, M.; Bacchetti, P.; Price, R. W.; Grant, R. M.; Schlote, W. HIV-related neuropathology, 1985 to 1999: rising prevalence of HIV encephalopathy in the era of highly active antiretroviral therapy. *J. Acquir. Immune Defic. Syndr.* **2002**, *31*, 171−177. (c) Nath, A.; Sinai, A. P. Cerebral toxoplasmosis. *Curr. Treat. Options Neurol.* **2003**, *5*, 3−12.
(9) (a) Horsburgh, C. R., Jr.; Gettings, J.; Alexander, L. N.; Lennox, J. L. Disseminated *Mycobacterium avium* complex disease among patients infected with human immunodeficiency virus. *Clin. Infect. Dis.* **2001**, *33*, 1938−1943. (b) Pozniak, A. Mycobacterial diseases and HIV. *J. HIV Ther.* **2002**, *7*, 13−16. (b) von Reyn, C. F.; Arbeit, R. D.; Horsburgh, C. R.; Ristola, M. A.; Waddell, R. D.; Tvaroha, S. M.; Samore, M.; Hirschhorn, L. R.; Lumio, J.; Lein, A. D.; Grove, M. R.; Tosteson, A. N. Sources of disseminated *Mycobacterium avium* infection in AIDS. *J. Infect.* **2002**, *44*, 166−170.
(10) Guerrant, R. L. Cryptosporidiosis: an emerging, highly infectious threat. *Emerg Infect Dis.* **1997**, *3*, 51−57. (b) Clark D. P. New insights into human cryptosporidiosis. *Clin Microbiol. Rev.* **1999**, *12*, 554−563. (c) Oldfield, E. C., III. Evaluation of chronic diarrhea in patients with human immunodeficiency virus infection. *Rev. Gastroenterol. Disord.* **2002**, *2*, 176−188.

(11) (a) Rosowsky, A.; Forsch, R. A.; Queener, S. F. Inhibition of *Pneumocystis carinii*, *Toxoplasma gondii*, and *Mycobacterium avium* dihydrofolate reductases by 2,4-diamino-5-[2-methoxy-5-(*ω*-carboxyalkyloxy)benzyl]pyrimidines: Marked improvement in potency relative to trimethoprim and species selectivity relative to piritrexim. *J. Med. Chem.* **2002**, *45*, 233−242. (b) Rosowsky, A.; Forsch, R. A.; Queener, S. F. Further studies on 2,4-diamino-5′-(2′, 5′-disubstituted benzyl)pyrimidines as potent and selective inhibitors of dihydrofolate reduces from three major opportunistic pathogens of AIDS. *J. Med Chem.* **2003**, *46*, 1726−1736; see this paper for a list of papers from this laboratory from 1993 to 2002.

(12) (a) Gangjee, A.; Dubash, N. P.; Queener, S. F. The synthesis of new diaminofuro[2,3-*d*]pyrimidines with 5-biphenyl, phenoxyphenyl and tricyclic substitutions as dihydrofolate reductase inhibitors. *J. Heterocycl. Chem.* **2000**, *37*, 935−942; see also many other papers from this group prior to 2000. (b) Gangjee, A.; Adair, O.; Queener, S. F. Synthesis of 2,4-diamino-6-(thioarylmethyl)pyrido[2,3-*d*]pyrimidines as dihydrofolate reductase inhibitors. *Bioorg. Med. Chem.* **2001**, *9*, 2929−2935. (c) Gangjee, A.; Zheng, Y.; McGuire, J. J.; Kisliuk, R. L. Synthesis of classical and nonclassical, partially restricted, linear, tricyclic 5-deazaantifolates. *J. Med. Chem.* **2002**, *45*, 5173−5181.

(13) (a) Piper, J. R.; Johnson, C. A.; Krauth, C. A.; Carter, R. L.; Hosmer, C. A.; Queener, S. F.; Borotz, S. E.; Pfefferkorn, E. R. Lipophilic antifolates as agents against opportunistic infections. 1. Agents superior to trimetrexate and piritrexim against *Toxoplasma gondii* and *Pneumocystis carinii* in in vitro evaluations. *J. Med. Chem.* **1996**, *39*, 1271−1280. (b) Suling, W. J.; Seitz, L. E.; Pathak, V.; Westbrook, L.; Barrow, E. W.; Zywnovan Ginkel, S.; Reynolds, R. C.; Piper, J. R.; Barrow, W. R. Antimycobacterial activities of 2,4-diamino-5-deazapteridine derivatives and effects on mycobacterial dihydrofolate reductase. *Antimicrob. Agents Chemother.* **2000**, *44*, 2784−2793.

(14) (a) Stevens, M. F. G.; Phillip, K. S.; Rathbone, D. L.; O'Shea, D. M.; Queener, S. F.; Schwalbe, C. H.; Lambert P. A. Structural studies on bioactive compounds. 28. Selective activity of triazenyl-substituted pyrimethamine derivatives against *Pneumocystis carinii* dihydrofolate reductase. *J. Med. Chem.* **1997**, *40*, 1886−1893. (b) Cody, V.; Chan, D.; Galitsky, N.; Rak, D.; Luft, J. R.; Pangborn, W.; Queener, S. F.; Laughton, C. A.; Stevens, M. F. G. Structural studies on bioactive compounds. 30. Crystal structure and molecular studies on the *Pneumocystis carinii* dihydrofolate reductase cofactor complex with TAB, a highly selective antifolate. *Biochemistry* **2000**, *39*, 3556−3564.

(15) Robson, C.; Meek, M. A.; Grunwaldt, J.-D.; Lambert, P. A.; Queener, S. F.; Schmidt, D.; Griffin, R. J. Nonclassical 2-diamino-5-aryl-6-ethylpyrimidine antifolates: Activity as inhibitors of dihydrofolate reductase from *Pneumocystis carinii* and *Toxoplasma gondii* and as antitumor agents. *J. Med. Chem.* **1997**, *40*, 3040−3048.

(16) For selected clinical examples, see: (a) Fischl, M. A.; Dickinson, G. M.; La Voie, L. Safety and efficacy of sulfamethoxazole and trimethoprim prophylaxis for *Pneumocystis carinii* pneumonia in AIDS. *J. Am. Med. Assoc.* **1988**, *259*, 1185−1189. (b) Medina, I.; Mills, H, Leuong, G.; Hopewell, P. C.; Lee, B.; Modin, G.; Benowitz, N.; Wofsy, C. B. Oral therapy for *Pneumocystis carinii* pneumonia in the acquired immunodeficiency syndrome. A controlled trial of trimethoprim-sulfamethoxazole versus trimethoprim-dapsone. *N. Engl. J. Med.* **1990**, *323*, 776−782. (c) Podzamczer, D.; Salazar, A.; Jimenez, J.; Consiglio, E.; Santin, M.; Casanova, A.; Rufi, G.; Gudiol, G. Intermittent trimethoprim-sulfamethoxazole compared with dapsone-pyrimethamine for the simultaneous primary prophylaxis of *Pneumocystis pneumonia* and toxoplasmosis in patients infected with HIV. *Ann. Intern. Med.* **1995**, *122*, 755−761. (d) Fraser, I.; Macintosh, I.; Wilkins, E. G. Prophylactic effect of co-trimoxazole for *Mycobacterium avium* complex infection: a previously unreported benefit. *Clin. Infect. Dis.* **1994**, *19*, 211.

(17) Roudier, C.; Caumes, E.; Rogeaux, O.; Bricaire, F.; Gentilini, M. Adverse cutaneous reactions to trimethoprim-sulfamethoxazole in patients with the acquired immunodeficiency syndrome and *Pneumocystis carinii* pneumonia. *Arch. Dermatol.* **1994**, *130*, 1383−1386.

(18) Ma, L.; Borio, L.; Masur, H.; Kovacs, J. A. *Pneumocystis carinii* dihydropteroate synthase but not dihydrofolate reductase gene mutations correlate with prior trimethoprim-sulfamethoxazole or dapsone use. *J. Infect. Dis.* **1999**, *180*, 1969−1978.

(19) (a) Sattler, F. R.; Frame, P.; Davis, R.; Nichols, L.; Shelton, B.; Akil, B.; Baughman, R.; Hughlett, C.; Weiss, W.; Boylen, C. T.; van der Horst, C.; Black, J.; Powderly, W.; Steigbigel, R. T.; Leedom, J. M.; Masur, H.; Feinberg, J.; Benoit, S.; Eyster, E.; Gocke, D.; Beck. K.; Lederman, M.; Phari, J.; Reichman, R.; Sacks, H. S.; Soiero, R.. Trimetrexate with leucovorin versus trimethoprim-sulfamethoxazole for moderate to severe episodes of *Pneumocystis carinii* pneumonia in patients with AIDS: a prospective, controlled multicenter investigation of the AIDS Clinical Trials Group Protocol 029/031. *J Infect. Dis.* **1994**, *170*, 165−172. (b) Fulton, B.; Wagstaff, A. J.; McTavish, D. Trimetrexate. A review of its pharmacodynamic and pharmacokinetic properties and therapeutic potential in the treatment of *Pneumocystis carinii* pneumonia. *Drugs* **1995** *49*, 563−576.

(20) Falloon, J.; Allegra, C. J.; Kovacs, J.; O'Neill, D.; Ogata-Arakaki, D.; Feuerstein, I.; Polis, M.; Davey, R.; Lane, H. C.; LaFon, S.; Rogers, M.; Zunich, K.; Turlo, J.; Tuazon, C.; Parenti, D.; Simon, G.; Masur, H. Piritrexim with leucovorin for the treatment of pneumocystis pneumonia (PCP) in AIDS patients. *Clin. Res.* **1990**, *38*, 361A.

(21) Kovacs, J. A.; Allegra, C. J.; Beaver, J.; Boarman, D.; Lewis, M.; Parrillo, J. E.; Chabner, B.; Masur, H. Characterization of de novo folate synthesis in *Pneumocystis carinii* and *Toxoplasma gondii*: Potential for screening therapeutic agents. *J. Infect. Dis.* **1989**, *160*, 312−320.

(22) Rosowsky, A.; Cody, V.; Galitsky, N.; Fu, H.; Papoulis, A. T.; Queener, S. F. Structure-based design of selective inhibitors of dihydrofolate reductase: synthesis and antiparasitic activity of 2,4-diaminopteridine analogues with a bridged diarylamine side chain. *J. Med. Chem.* **1999**, *42*, 4853−4860.

(23) Cody, V.; Galitsky, N.; Luft, J. R.; Pangborn, W.; Rosowsky, A.; Queener, S. F. Structure-based enzyme inhibitor design: modeling studies and crystal structure analysis of *Pneumocystis carinii* dihydrofolate reductase ternary complex with PT653 and NADPH. *Acta Crystallogr.* **2002**, *D58*, 946−954.

(24) Rosowsky, A.; Fu, H.; Queener, S. F. Synthesis of new 2,4-diaminopyrido[2,3-*d*]pyrimidines and 2,4-diaminoquinazolines with bulky dibenz[*b*,*f*]azepine and dibenzo[*a*,*d*]cycloheptene substituents at the 6-positiion as inhibitors of dihydrofolate reductases from *Pneumocystis carinii*, *Toxoplasma gondii*, and *Mycobacterium avium*. *J. Heterocycl Chem.* **2000**, *37*, 921−926.

(25) Haque, K. H.; Hardie, K. M.; Proctor, G. R. Novel aromatic systems. Part IX. Synthesis and substitutions of dibenzo[*b*,*f*]-azepin-2-one. *J. Chem. Soc., Perkin Trans. 1* **1972**, 539−542.

(26) Chang, V. H. T. Synthesis of 2-hydrocycarbamazepine. A metabolite of carbam-azepine. *J. Heterocycl. Chem.* **1983**, *20*, 237−238.

(27) (a) Stadler, P. A.; Frey, A. J.; Troxler, R.; Hofmann, A. Selective reduction and oxidation reactions of lysergic acid derivates. *Helv. Chim. Acta* **1964**, *47*, 756−769. (b) Saa, J. M.; Capo, M.; Marti, C.; Garcia-Raso, A. Oxidative degradation of 6-hydroxy-1,2,3,4-tetrahydroisoquinolines and 7-hydroxy-2-benazepines. A novel route to heterocyclic quinones. *J. Org. Chem.* **1990**, *55*, 288−292. (c) Islam, L.; Skibo, E. B.; Dorr, R. T.; Alberts, D. S. Structure−activity studies of antitumor agents based on pyrrolo-[1,2-*a*]benzimidazoles: New reductive alkylating DNA cleaving agents. *J. Med. Chem.* **1991**, *34*, 2954−2961. (d) Giethlen, B.; Schaus, J. M. Oxidation of indolines with Fremy's salt: A mechanistic proposal. *Tetrahedron Lett.* **1997**, *38*, 3483−3486. (d) Kraus, G. A.; Selvakumar, N. A novel Fremy's salt-mediated oxidation and rearrangement of anilines into amino orthodiketones. Applications to the synthesis of pyrrolobenzodiazepines. *Tetrahedron Lett.* **1999**, *40*, 2039−2040.

(28) Taylor, E. C.; Portnoy, R. C.; Hochstetler, D. C.; Kobayashi, T. Pteridines. XXXVIII. Synthesis of some 2,4-diamino-6-substituted methylpteridines. A new route to pteroic acid. *J. Org. Chem.* **1975**, *40*, 2347−2351.

(29) Rosowsky, A.; Forsch, R. A.; Queener, S. F.; Bertino, J. R. Synthesis of 2,4-diaminopteridines with bulky lipophilic groups at the 6-position as inhibitors of *Pneumocystis carinii*, *Toxoplasma gondii*, and mammalian dihydrofolate reductase. *Pteridines* **1997**, *8*, 173−187.

(30) Kuyper, L. F.; Roth, B.; Baccanari, D. P.; Ferone, R.; Beddell, C. R.; Champness, J. N.; Stammers, D. K.; Dann, J. G.; Norrington, F. E.; Baker, D. J.; Goodford. P. J. Receptor-based design of dihydrofolate reductase inhibitors: comparison of crystallographically determined enzyme binding with enzyme affinity in a series of carboxy-substituted trimethoprim analogues. *J. Med. Chem.* **1985**, *28*, 303−311.

(31) Broughton, M. C.; Queener, S. F. *Pneumocystis carinii* dihydrofolate reductase used to screen potential antipneumocystis drugs. *Antimicrob. Agents Chemother.* **1991**, *35*, 1348−1355.

(32) Chio, L.-C.; Queener, S. F. Identification of highly potent and selective inhibitors of *Toxoplasma gondii* dihydrofolate reductase. *Antimicrob. Agents Chemother.* **1993**, *37*, 1914−1923. Note that in our original paper in which the activity of **6** against *T. gondii* tachyzoites was reported[22] the reference cited for the [^{3}H]-uracil incorporation assay method should have been 16b instead of 17c.

(33) Then, R. L.; Hartman, P. G.; Kompis, I.; Stephan-Güldner, M.; Stöckel, K. Epiroprim. *Drugs Future* **1994**, *19*, 446−449.

(34) Gangjee, A.; Vasudevan, A.; Queener, S. F.; Kisliuk, R. L. 2,4-Diamino-5-deaza-6-substituted pyrido[2,3-*d*]pyrimidine antifolates as potent and selective nonclassical inhibitors of dihydrofolate reductases. *J. Med. Chem.* **1996**, *39*, 1438−1446.

(35) Wang, Y.; Bruenn, J. A.; Queener, S. F.; Cody, V. Isolation of rat dihydrofolate reductase gene and characterization of recombinant enzyme. *Antimicrob. Agents Chemother.* **2001** *45*, 2517−

2523. Note that the SI of compound **6**, referred to as PT653 in this paper, was inadvertently listed as 1.9, instead of 13.9 for Pc versus human DHFR. However, as evident from the IC_{50} values and the accompanying discussion, the potency and selectivity of **6** for Pc versus human and for Pc versus rat DHFR are very similar.

(36) Structural studies on rat DHFR by crystallography are in progress in the laboratory of Dr. Vivian Cody, Hauptman-Woodward Medical Research Institute, Buffalo, NY.

(37) For computational studies on the set of pyrido[2,3-*d*]pyrimidine analogues synthesized by Suling and co-workers,[13b] as well as our lead compound **6**, see: Debnath, A. K. Pharmacophore mapping of a series of 2,4-diamino-5-deazapteridine inhibitors of *Mycobacterium avium* complex dihydrofolate reductase, see *J. Med. Chem.* **2002**, *45*, 41−53. For a more recent modeling study in which several of these structures were docked into a homology model of Ma DHFR derived from a published 3D structure for *Mycobacterium tuberculosis* DHFR, see: Kharkar, P. S.; Kulkarni, V. M. A proposed model of *Mycobacterium avium* complex dihydrofolate reductase and its utility for drug design. *Org. Biomol. Chem.* **2003**, *1*, 1315−1322.

(38) (a) Dhople, A. L. In vitro activity of epiroprim, a dihydrofolate reductase inhibitor, singly and in combination with brodimoprim and dapsone, against *Mycobacterium leprae*. *Int. J. Antimicrob. Agents* **1999**, *12*, 319−323. (b) Dhople, A. L. Antimicrobial activities of dihydrofolate reductase inhibitors, used singly or in combination with dapsone, against *Mycobacterium ulcerans*. *J. Antimicrob. Chemother.* **2001**, *47*, 93−96.

(39) Tripos, Inc., St. Louis, MO.

(40) In the discussion of the interactions of **10** with Pc and human DHFR, the ring to which the 2′-substituent is attached is called the A-ring, the azepine ring is called the B-ring, and the third ring in the tricyclic system is called the C-ring.

(41) Andrews, P.; Dooley, M. Role of molecular recognition in drug design. In: *Textbook of Drug Design and Discovery*, 3rd ed.; Krogsgaard-Larsen, P., Liljefors, T., Madsen, U., Eds.; Taylor and Francis Publishers: London, UK, 2000; pp 35−53.

(42) (a) Cody, V.; Rosowsky, A. Crystal structure determination of human DHFR binary complexes with TMP and modeling studies of TMP analogues. *AACR Proc.* **2002**, *43*, 1021. (b) Personal communication from Dr. Vivian Cody.

(43) Case, D. A.; Pearlman, D. A.; Caldwell, J. W.; Cheatham, T. E., III; Wang, J.; Ross, W. S.; Simmerling, C. L.; Darden, T. A.; Merz, K. M.; Stanton, R. V.; Cheng, A. L.; Vincent, J. J.; Crowley, M.; Tsui, V.; Gohlke, H.; Radmer, R. J.; Duan, Y.; Pitera, J.; Massova, l.; Seibel, G. L.; Singh, U. C.; Weiner, P. K.; Kollman, P. A. AMBER 7; University of California, San Francisco, 2002.

(44) Wang, J.; Cieplak, P.; Kollman, P. A. How well does a restrained electrostatic potential (RESP) model perform in calculating conformational energies of organic and biological molecules? *J. Comput. Chem.* **2000**, *21*, 1049−1074.

(45) Cornell, W.; Cieplak, P.; Bayly, C.; Gould, I.; Merz, K.; Ferguson, D.; Spellmeyer, D.; Fox, T.; Caldwell, J.; Kollman, P. A. A second generation force field for the simulation of proteins, nucleic acids, and organic molecules. *J. Am. Chem. Soc.* **1995**, *117*, 5179−5197.

(46) Jakalian, A.; Bush, B. L.; Jack, D. B.; Bayly, C. I. Fast, efficient generation of high-quality atomic charges. AM1-BCC Model: I. Methodol. *J. Comput. Chem.* **2000**, *21*, 132−146.

(47) Stewart, J. J. P. Rossi, I.; Hu, W. P.; Lynch, G. C.; Liu, Y. P.; Chuang, Y. Y.; Li, J.; Cramer, C. J.; Fast, P. L.; Truhlar, D. G. MOPAC version 5.09mn; University of Minnesota, Minneapolis, 1999.

(48) Cody, V.; Galitsky, N.; Luft, J. R.; Pangborn, W.; Rosowsky, A.; Blakley, R. L. Comparison of two independent crystal structures of human dihydrofolate reductase ternary complexes with reduced nicotinamide adenine dinucleotide phosphate and the very tight-binding inhibitor PT523. *Biochemistry* **1997**, *36*, 13897−13903.

(49) Ryckaert, J.; Ciccoti, G.; Berendsen, H. Numerical integration of the Cartesian equations of motion for a system of constraints. *J. Comput. Phys.* **1977**, *23*, 327−341.

JM030599O